



# Stratospheric ozone in boreal fire plumes – the 2013 smoke season over central Europe

T. Trickl<sup>1</sup>, H. Vogelmann<sup>1</sup>, H. Flentje<sup>2</sup>, and L. Ries<sup>3</sup>

<sup>1</sup>Karlsruher Institut für Technologie, Institut für Meteorologie und Klimaforschung (IMK-IFU), Kreuzeckbahnstr. 19, 82467 Garmisch-Partenkirchen, Germany

<sup>2</sup>Meteorologisches Observatorium Hohenpeißenberg des Deutschen Wetterdienst, Albin-Schwaiger-Weg 10, 82383 Hohenpeißenberg, Germany

<sup>3</sup>Umweltbundesamt II 4.5, Plattform Zugspitze, GAW-Globalobservatorium Zugspitze-Hohenpeißenberg, Schneefernerhaus, 82475 Zugspitze, Germany

Correspondence to: T. Trickl (thomas.trickl@kit.edu)

Received: 22 March 2015 – Published in Atmos. Chem. Phys. Discuss.: 6 May 2015

Revised: 19 August 2015 – Accepted: 20 August 2015 – Published: 28 August 2015

**Abstract.** In July 2013 very strong boreal fire plumes were observed at the northern rim of the Alps by lidar and ceilometer measurements of aerosol, ozone and water vapour for about 3 weeks. In addition, some of the lower-tropospheric components of these layers were analysed at the Global Atmosphere Watch laboratory at the Schneefernerhaus high-altitude research station (2650 m a.s.l., located a few hundred metres south-west of the Zugspitze summit). The high amount of particles confirms our hypothesis that fires in the Arctic regions of North America lead to much stronger signatures in the central European atmosphere than the multitude of fires in the USA. This has been ascribed to the prevailing anticyclonic advection pattern during favourable periods and subsidence, in contrast to warm-conveyor-belt export, rain-out and dilution frequently found for lower latitudes. A high number of the pronounced aerosol structures were positively correlated with elevated ozone. Chemical ozone formation in boreal fire plumes is known to be rather limited. Indeed, these air masses could be attributed to stratospheric air intrusions descending from remote high-latitude regions, obviously picking up the aerosol on their way across Canada. In one case, subsidence from the stratosphere over Siberia over as many as 15–20 days without increase in humidity was observed although a significant amount of Canadian smoke was trapped. These coherent air streams lead to rather straight and rapid transport of the particles to Europe.

## 1 Introduction

The increase of tropospheric ozone during the past decades has been frequently attributed to a growth in anthropogenic air pollution. However, this development has recently continued only in rapidly developing regions such as in eastern Asia. In Europe the ozone precursors considerably diminished in the 1990s (e.g., Jonson et al., 2006; Vautard et al., 2006; and references therein).

There is growing evidence that natural ozone sources cannot be neglected, and there have been hints that, e.g., ozone import from the stratosphere could be quite considerable (e.g., Roelofs and Lelieveld, 1997). In fact, measurements at high-altitude stations in Europe such as Jungfraujoch (Switzerland, 3500 m a.s.l.) and Zugspitze (Germany, 2962 m a.s.l.) have shown growing ozone concentrations even more than a decade after the onset of diminishing anthropogenic ozone precursor concentrations (e.g., Cui et al., 2011; Oltmans et al., 2012). Scheel (2003, 2005) identified an increase of the most important natural source of ozone, stratosphere-to-troposphere transport (STT), to be responsible for the increase in Zugspitze ozone (see also Ordoñez et al., 2007, for the Jungfraujoch station). Scheel (2005) also found that the role of STT for the Zugspitze site has been grossly underestimated, with an estimated average STT fraction of about 40 % reached by 2004. Another strong source of STT previously underestimated was emphasized by Sprenger

et al. (2003): vertical exchange along the subtropical jet stream (see also Škerlak et al., 2014).

It is interesting to note that the nearby lidar measurements at Garmisch-Partenkirchen have rarely shown major ozone peaks of other than stratospheric origin in recent years, in contrast to the situation over 1 decade ago (e.g., Stohl and Trickl, 1999; Stohl et al., 2003; Trickl et al., 2003; Huntrieser et al., 2005; Roelofs et al., 2003). This could be a sign of improving air quality in the Northern Hemisphere, except for eastern Asia.

Another natural source of ozone is biomass burning. Fire maps obtained from satellite-borne measurements show an enormous coverage of the globe by natural and anthropogenic fires. The role of biomass burning can become even more severe on the way to a warmer climate. In fact, the area burnt in the USA has roughly doubled since the 1990s (e.g., Fig. 2 in Trickl et al., 2013). The potentially growing role of high-reaching fire events occasionally even penetrating into the lower stratosphere, so-called pyrocumulonimbus plumes, has been discussed by e.g., Fromm and Servranckx (2003) and Fromm et al. (2000, 2008a, b, 2010).

The lidar measurements at Garmisch-Partenkirchen, in particular within the EARLINET (European Aerosol Research Lidar Network; Bösenberg et al., 2003) project and during the intense routine measurements in recent years, have never shown strong fire signatures from the USA. However, several cases of spectacular plumes from fires in Arctic regions have been observed here and at other places in central Europe (e.g., Forster et al., 2001; Mattis et al., 2003; Damoah et al., 2004; pp. 58–59 in ATMOFAST, 2005; Petzold et al., 2007). This has led us to the idea that the transport from lower latitudes in North America to Europe is less coherent or is implying a partial washout of particles in warm-conveyor belts (see also Birmili et al., 2010).

There is agreement that biomass burning leads to ozone formation. Numerous investigations of the atmospheric impact of tropical fires have given clear evidence that elevated levels of ozone over South America and Africa are due to the excessive burning of forests and savannah, the rain forest otherwise acting as an important net sink for ozone (e.g., Delany et al., 1985; Browell et al., 1988; Gregory et al., 1988; Crutzen and Andreae, 1990; Richardson et al., 1991; Kirchhoff and Marinho, 1994; Kirchhoff, 1996; Kirchhoff et al., 1996). A retrieval of satellite measurements has given evidence of substantial ozone export to the tropical oceanic regions (Fishman et al., 1986; Fishman and Larsen, 1987), a strong burden to the otherwise clean troposphere in the Southern Hemisphere during certain periods of the year. The tropospheric ozone formation is  $\text{NO}_x$  limited, with the hydrocarbon-to- $\text{NO}_x$  ratios varying between roughly 15 and 150, the latter value corresponding to boreal fires (Jaffe and Widger, 2012).

In fact, substantially less ozone formation is expected for boreal fires. For instance, Alvarado et al. (2010) verified rapid conversion of  $\text{NO}_x$  into PAN (peroxyacetyl nitrate) in a

boreal forest fire plume over Canada. The lower relative  $\text{NO}_x$  content in boreal fires, together with the lower solar elevation angle, can be seen as the reason for the much slower build-up of ozone in fire plumes originating in high-latitude regions.

The build-up of ozone during long-range transport reaching lower latitudes has been ascribed mainly to thermal decomposition of PAN (e.g., Jacob et al., 1992). For instance, Real et al. (2007) investigated the role of this mechanism to understand ozone formation from intense fire plumes from Alaska and Canada on the way from America to Europe in a modelling case study based on measurements during the 2004 ICARTT (International Consortium for Atmospheric Research on Transport and Transformation) Lagrangian field campaign (Fehsenfeld et al., 2006). During the same field campaign, Val Martin et al. (2006) observed enhanced ozone in the boreal fire plumes reaching the Azores Islands.

Another reason for the coexistence of enhanced ozone and smoke could be the mixing of air from the biomass burning plume and stratospheric air (Brioude et al., 2007). Also, parts of the 2004 ICARTT boreal plumes proceeded within a layer descending from the tropopause region (Methven et al., 2006; Real et al., 2007). On the other hand, we have rarely seen strong mixing of stratospheric and tropospheric air in our lidar results (Trickl et al., 2014).

In this paper, we report on observations of long-lasting biomass burning plumes from mainly Canada and Alaska in the Garmisch-Partenkirchen area (German Alps) in July 2013. The observations comprise lidar measurements of ozone, water vapour, and aerosol; ceilometers capturing complete time series of information on the particles around the clock under clear-sky conditions; and measurements of specific chemical tracers at the Schneesfernerhaus high-altitude station.

## 2 Methods

### 2.1 Lidar systems

The tropospheric ozone lidar is operated in Garmisch-Partenkirchen, Germany (IMK-IFU;  $47^\circ 28' 37''$  N,  $11^\circ 3' 52''$  E, 740 m a.s.l.). The laser source is a narrow-band Raman-shifted KrF laser, and two separate receiving telescopes are used to divide the dynamic range of the backscatter signal of roughly 8 decades. This lidar was first completed as a two-wavelength differential-absorption lidar (DIAL) in 1990 (Kempfer et al., 1994). It was later upgraded to a three-wavelength DIAL in 1994 and 1995 (Eisele and Trickl, 1997, 2005), leading to a unique vertical range between roughly 0.3 km above the ground and 3–5 km above the tropopause, the measurement time interval being just 41 s. It features low uncertainties of about  $\pm 3$  ppb in the lower free troposphere, increasing up to  $\pm 6$  ppb (under optimum conditions) in the upper troposphere. The uncertainty further diminished after another system

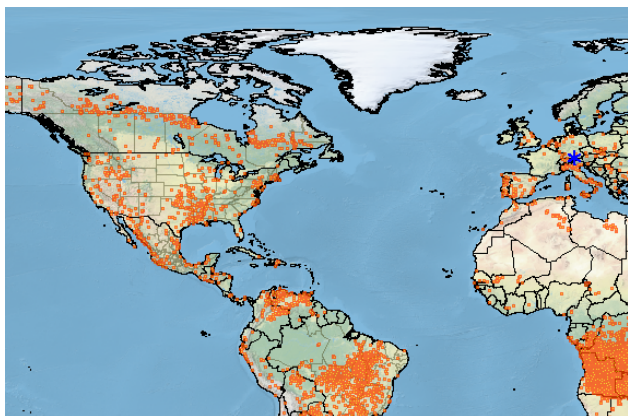


**Figure 1.** Fire spots between 1 and 7 July 2013, as generated by the FIRMS Web Fire Mapper: A “road of fire” formed west to east across Canada along the most frequent backward trajectory pathways initiated over Garmisch-Partenkirchen. The position of Garmisch-Partenkirchen is marked by a blue asterisk.

upgrading in 2012 that resulted in noise reduction by more than a factor of 3. For the range covered by the near-field receiver (below 1.2 km above the lidar), the uncertainty is of the order of  $\pm 6$  ppb. Comparisons with the Zugspitze in situ ozone measurements show no relevant mutual bias, the standard deviation of the differences being less than 2 ppb. The upper-tropospheric performance may be degraded in the presence of high lower-tropospheric ozone concentrations absorbing a lot of the ultraviolet laser emission and by enhanced sky light in summer, particularly in the presence of clouds. Thus, longer data acquisition times, requiring some technical modifications, are planned for the future. The vertical resolution is dynamically varied between 50 m and a few hundred metres, depending on the signal-to-noise ratio decreasing with altitude. The lidar has been used in numerous atmospheric transport studies (e.g., Eisele et al., 1999; Seibert et al., 2000; Carnuth et al., 2002; Trickl et al., 2003, 2010, 2011, 2014; Zanis et al., 2003).

The Oberschleißheim (“Munich”, station number 10868) radiosonde data have been used for calculating the atmospheric density and, subsequently, both the ozone mixing ratio and the Rayleigh optical coefficients. If no Munich data are available the listings for Stuttgart (station number 10739) have been taken.

Backscatter coefficients are calculated from the “off” channel of the ozone DIAL (313.2 nm). The quality of these data and the sensitivity for small amounts of aerosol has, since 2012, also greatly improved due to the lower noise. Structures in the backscatter coefficients of less than  $5 \times 10^{-8} \text{ m}^{-1} \text{ sr}^{-1}$ , corresponding to an aerosol-related standard visual range (as defined in VDI, 2004: attenuation of the radiation to 2 %) of more than 1500 km, can be resolved. This performance motivated us to store the 313 nm aerosol data in the database of the European Aerosol Research Lidar Net-

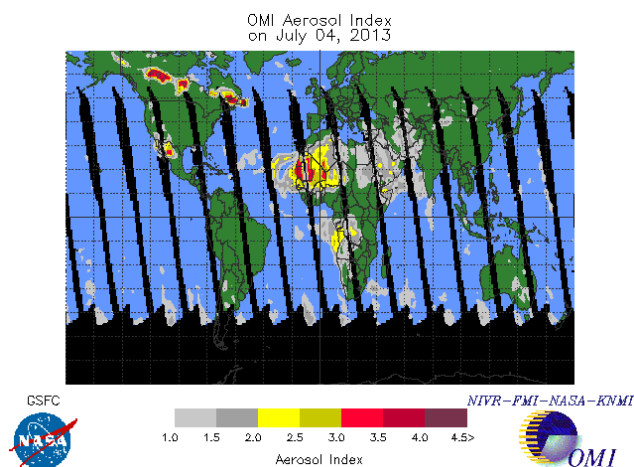


**Figure 2.** OMI aerosol index for 4 July 2013.

work (EARLINET) since November 2012. The backscatter profiles are corrected for radiation loss in ozone. A constant backscatter-to-extinction ratio  $B_p = 0.020 \text{ m}^{-1} \text{ sr}^{-1}$  is used as obtained for average European continental aerosol (Pappalardo, 2003; see also, e.g., Mattis et al., 2004, and Amiridis et al., 2005). This value is also applicable to aged fire aerosol (Müller et al., 2005 (355 nm); further information in Müller et al., 2007). Some uncertainties arise from our own assessment for 313 nm: in the past we obtained  $0.03 \text{ m}^{-1} \text{ sr}^{-1}$  for this wavelength from measurements revealing homogeneous aerosol distributions (Eisele and Trickl, 2005). However, the difference rarely amounts to more than 10 % for the backscatter coefficients, due to the typical low-to-moderate-extinction conditions above our site. For clouds  $B_p$  was typically varied between 0.03 and  $0.10 \text{ m}^{-1} \text{ sr}^{-1}$  for a smooth transition of the extended Klett (1985) retrieval from above to below the cloud range. This variability is very likely to be due to the transient nature of clouds that are frequently just partly present during the measurement period.

Around aerosol layers the ozone profiles have been corrected as described by Eisele and Trickl (2005). The coefficients describing the wavelength dependences were varied to ensure that the correction is robust. In the presence of particles the wavelength combination 277–292 nm was used for the ozone retrieval wherever possible. This combination exhibits a rather low sensitivity with respect to aerosol (Völger et al., 1996; Eisele and Trickl, 2005).

The water-vapour DIAL is operated at the Schneefernerhaus high-altitude research station at 2675 m a.s.l., about 8.5 km to the south-west of IMK-IFU, 0.7 km to the south-west of and about 300 m below the Zugspitze summit (2962 m a.s.l.). The full details of this lidar system were described by Vogelmann and Trickl (2008). This lidar system is based on a powerful tunable narrow-band Ti:sapphire laser system with up to 250 mJ (typical choice: 100 mJ) energy per pulse operated at about 817 nm and a 0.65 m diameter New-

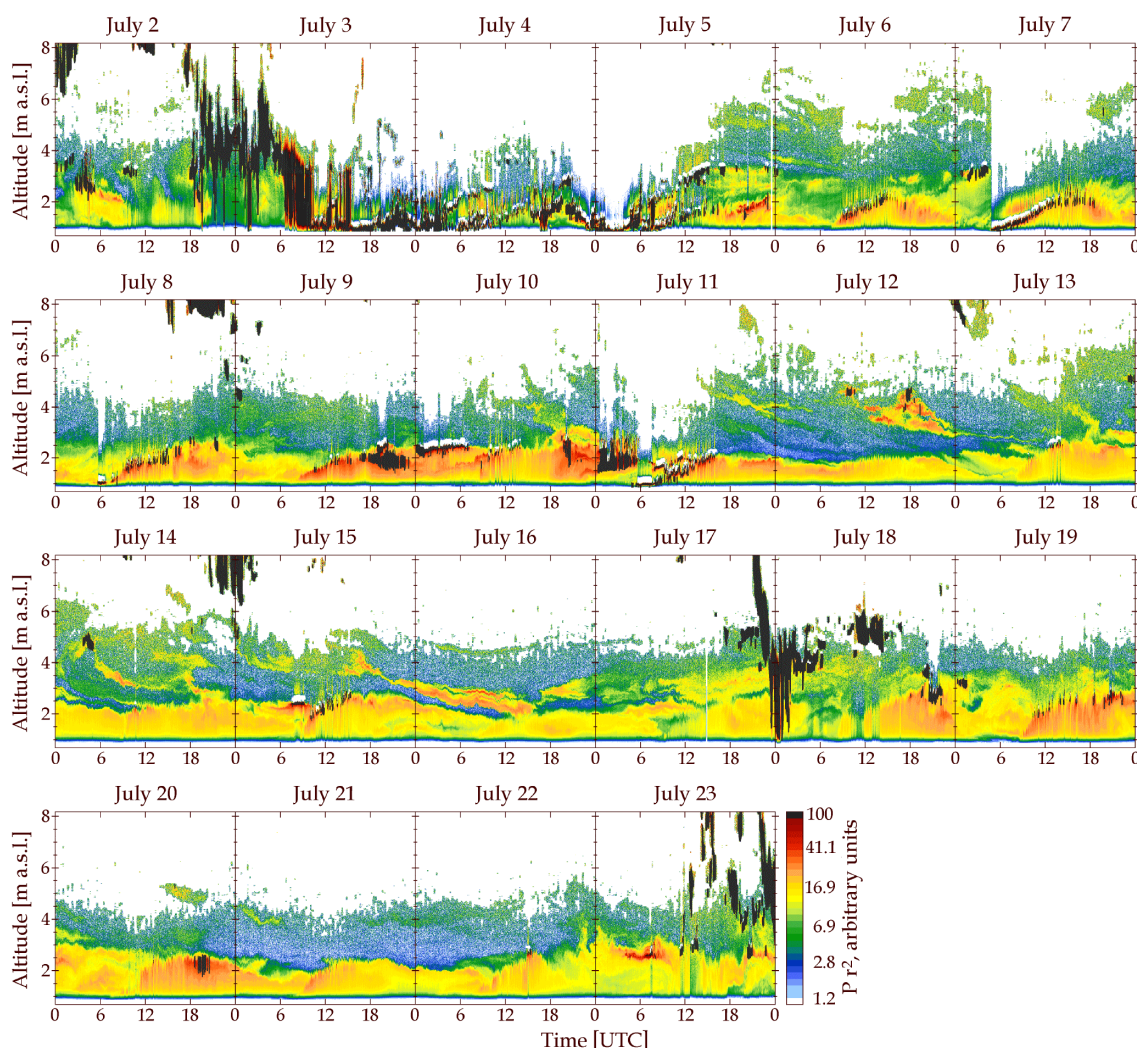


**Figure 3.** Range-corrected backscatter signal ( $P(r)r^2$ ; logarithmic colour code) measured by ceilometer over Leutkirch (southern Germany) from 2 to 23 July 2013. Areas with low signal-to-noise ratio are masked white. On several days the Canadian smoke layers filled a considerable part of the free troposphere above the mixing layer (up to 2 km, marked by yellow to reddish colour).

tonian receiver. Due to these specifications a vertical range of up to about 12 km is achieved, almost independent of the daylight, with measurement durations of about 15 min. The vertical resolution chosen in the data evaluation is dynamically varied between 50 m in altitude regions with good signal-to-noise ratio and roughly 260 m in the upper troposphere. Under optimum conditions the noise limit above 10 km a.s.l. corresponds to uncertainties of about  $\pm 1.5 \times 10^{20} \text{ m}^{-3}$  (density) or about 18 ppm (volume mixing ratio). In the lowermost part of the operating range (3–4 km) we estimate a density noise limit of  $\pm 5 \times 10^{20} \text{ m}^{-3}$  or roughly  $\pm 25$  ppm for layers with very low humidity and a relative uncertainty of about 5 % under more humid conditions. Free-tropospheric measurements under dry conditions clearly benefit from the elevated site outside or just below the edge of the moist Alpine boundary layer (e.g., Carnuth and Trickl, 2000; Car-

nuth et al., 2002). After a few years of testing, validating and optimizing the system, routine measurements were started in January 2007 with typically 2 measurement days per week, provided that the weather conditions are favourable. During this period, successful comparisons with an air-borne DIAL and a ground-based Fourier-transform infrared spectrometer (Wirth et al., 2009; Vogelmann et al., 2011, 2015) were also achieved, verifying average mutual biases of not more than 1 %. The lidar is capable of resolving the concentrations in extremely dry layers of stratospheric origin in the lower free troposphere of the order of 25 ppm  $\text{H}_2\text{O}$  (Trickl et al., 2014).

## 2.2 Ceilometers

The dispersion and temporal development of the North American smoke plumes is visualized by ceilometer measurements of the German Weather Service (DWD) network

(<http://www.dwd.de/ceilomap>). DWD operates more than 60 Lufft (<http://www.lufft.com/>) CHM15k ceilometers in Germany (Flentje et al., 2010) and provides series of operational range-corrected particle backscatter profiles ( $P(r)r^2$  “quick-look” graphics,  $P$  being the particle backscatter signal and  $r$  the distance from the lidar). Two-dimensional time-height sections of  $P(r)r^2$  show development and dispersion of the mixing layer, clouds, and aerosols like the Canadian fire plumes in July 2013. The CHM15k uses a diode-laser-pumped Nd:YAG (neodymium-doped yttrium aluminium garnet) solid state laser emitting at 1064 nm and covers altitudes from about 0.3 to 15 km above ground (Heese et al., 2010). A reasonable resolution for aerosol profiles is 100 m in the vertical and 5 min in time. The IR (infrared) wavelength is more sensitive to particles larger than 1  $\mu\text{m}$  and limits Rayleigh calibration capability, but system stability and upgraded performance tracking allows for absolute calibration (Wiegner and Geiß, 2012) to infer attenuated backscatter profiles (not used here).

The data from three DWD ceilometer stations have been inspected for this study, Schneefernerhaus, Hohenpeißenberg (48 km north of Garmisch-Partenkirchen, a DWD mountain observatory (summit: 988 m a.s.l.) outside the Alps), and Leutkirch (about 85 km west-north-west of Garmisch-Partenkirchen, outside the Alps). Schneefernerhaus was frequently within clouds, the least cloud-affected site during the period of interest was Leutkirch.

### 2.3 In situ instrumentation

On several occasions a fire plume directly hit the Zugspitze summit and could also be at least partly observed at the Global Atmosphere Watch (GAW) laboratory at the Schneefernerhaus research station (UFS; see H<sub>2</sub>O lidar), operated by the German Umweltbundesamt (UBA; i.e., Federal Environmental Agency; 47°25′0″ N, 11°58′46″ E; air inlet at 2670 m a.s.l.). Species of relevance for this study measured at UFS are ozone, carbon monoxide, NO<sub>y</sub>, PM<sub>10</sub>, equivalent black carbon and condensation nuclei. The NO<sub>y</sub> measurements were not reliable during the period discussed here because of a newly installed NO<sub>y</sub> gold converter and were, thus, not included in the analysis.

The inlet for reactive gases – ozone, carbon monoxide and nitrogen oxides – consists of a stainless-steel tubing with diameter of approximately 14 cm with an inlay tubing of borosilicate glass. This prevents the sample from direct contact with the metal surface and, therefore, chemical modification. The flow rate in the glass system is 500 L min<sup>-1</sup>. The inlet for aerosols consists of stainless steel, which protects the collected aerosols from side effects due to static electricity, which would occur at glass surfaces. The flow rate in the steel system supports a laminar flow of 100 L min<sup>-1</sup>.

Ozone is continuously measured by ultraviolet (UV) absorption at 254 nm (Thermo Electron Corporation, model

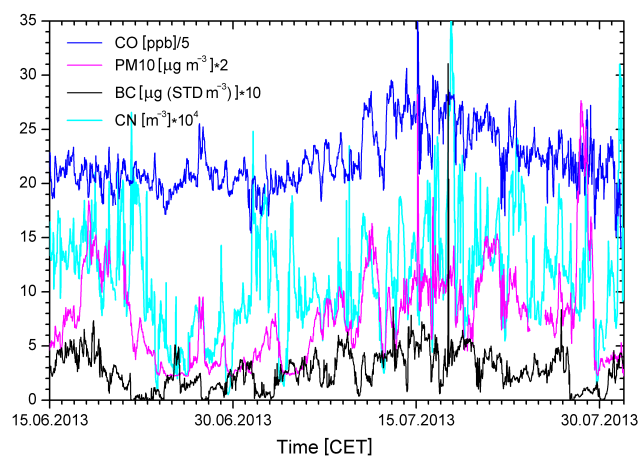


**Figure 4.** Overview of selected species measured at UFS between 15 June and 1 August 2013: during the fire period in July elevated CO was observed parallel to the increase in particles, which had not been the case in June. BC means black carbon, and CN condensation nuclei.

Ts49i). CO is determined from UV fluorescence excited by a CO resonance lamp (Aero-Laser, fast model 5002).

Aerosol with an aerodynamic diameter  $\leq 10 \mu\text{m}$  (PM<sub>10</sub>) is measured with a combination of absorption of  $\beta$  radiation for higher concentration ranges and a nephelometer for lower concentration ranges, integrated in the same instrument (Thermo Scientific, Sharp, model 5030). The increase of  $\beta$  absorption measured for a time increment, caused by the increase of PM<sub>10</sub> which has settled during this time on a filter paper, is used in combination with the measured aerosol light scattering for the determination of the PM<sub>10</sub> mass increment, measured during the same time step. The mass increment of black carbon (elemental carbon) on a glass-fiber filter belt is determined by absorption photometry in reflectometric measurements applying various diffraction angles (Thermo Scientific, model 5012). The final measurement of light transmission also takes into account multiple light scattering.

The calibration of the UBA instrumentation is routinely verified as a part of the GAW quality assurance efforts. The instruments are controlled daily and serviced on all regular work days and calibrated at intervals ranging between once every 3 days, weekly or monthly, depending on the type of instrument. The calibration standards for NO and ozone are directly linked to the German standard, which is transferred by the reference lab for experimental analysis of air quality of the German Federal Environment Agency via BIPM (Bureau International des Poids et Mesures), Paris, which itself is adjusted with the NIST (National Institute of Standards and Technology, USA).

No measurements have been available from the Zugspitze summit station of IMK-IFU (e.g. Logan et al., 2012; Oltmans et al., 2012; Parrish et al., 2012) because the in situ measurements of IMK-IFU at this station have been discon-

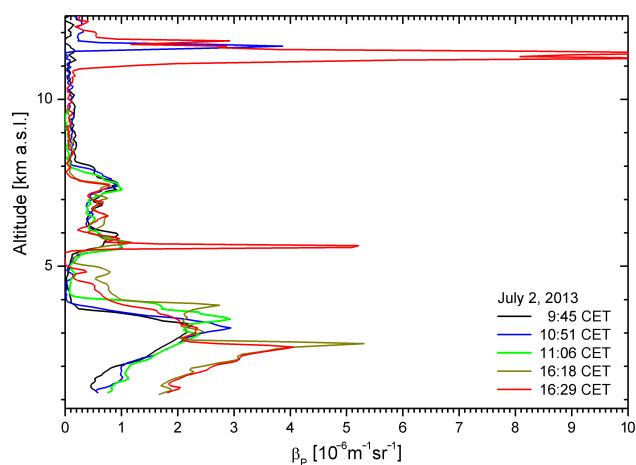


**Figure 5.** 313 nm particle backscatter coefficients for 2 July 2013; the spikes between 11 and 12 km are due to faint cirrus clouds.

tinued since 2013, after the retirement of H. E. Scheel. The Zugspitze aerosol instrumentation was also not available during the period discussed in this paper.

## 2.4 Analysis tools

For the identification of the transport pathways we have extensively used HYSPLIT (Draxler and Hess, 1998; <http://ready.arl.noaa.gov/HYSPLIT.php>) 315 h backward trajectory calculations (three-dimensional (“model vertical velocity”), based on re-analysis meteorological data). Although the re-analysis data seem to be coarser than other meteorological data available they have shown a superior performance in the free troposphere in many of our studies (Trickl et al., 2010, 2013, 2014; Fromm et al., 2010) and the analysis of our routine measurements. Despite the known limitations of backward trajectories (e.g., Stohl and Seibert, 1998) most specific free-tropospheric layers in years of observations could be related to reasonable sources with this operation mode of HYSPLIT, the best investigated transport type being STT. In the study presented here both normal and ensemble trajectories have been calculated. Although there is mostly some spread of the trajectories over boreal North America, those started in or around a smoke layer detected with the lidar systems pass over the fire regions described in Sect. 3. Because of the reproducibility of this behaviour we just give a few examples of our trajectory calculations for illustration and for clearness select normal trajectories.

In addition, images of satellite data have been systematically inspected, such as aerosol maps of the Ozone Monitoring Instrument (OMI) or the aerosol images from the spaceborne lidar CALIOP (Cloud-Aerosol Lidar with Orthogonal Polarization) onboard the CALIPSO (Cloud-Aerosol Lidar and Infrared Pathfinder Satellite Observation) satellite (<http://www-calipso.larc.nasa.gov/>).

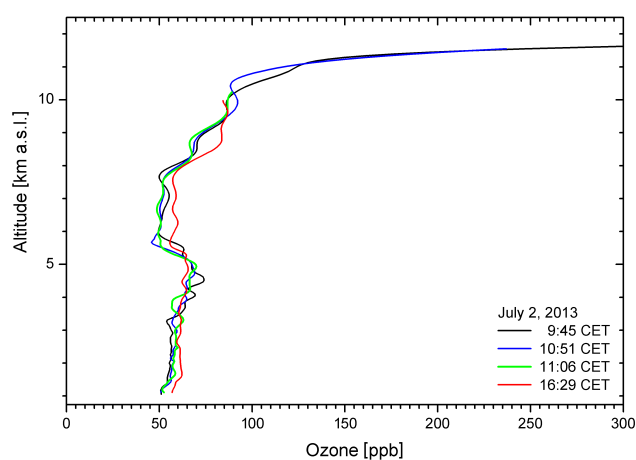


**Figure 6.** Ozone mixing ratios for 2 July 2013; please note the moderate mixing ratio in the fire plume ranges between about 5.5 and 8 km.

For days without measurements with the water-vapour DIAL, relative-humidity (RH) data of surrounding radiosonde stations have been inspected (e.g., Payerne, station number 06610, 315 km to the west; Stuttgart, station number 10739, 215 km to the north-west; Oberschleißheim, “Munich”, station number 10868, 100 km roughly to the north; Kümmersbruck, station number 10771, 210 km roughly to the north; Graz, station number 11240, 330 km roughly to the south-east), as well as from others not discussed in this paper. The choice of the station is based on the trajectories.

## 3 The North American fire situation in June and July 2013

The 2013 fires in North America could be conveniently tracked on a day-by-day basis from the FIRMS (Fire Information for Resource Management System, <https://earthdata.nasa.gov/data/near-real-time-data/firms>) Web Fire Mapper (<https://firms.modaps.eosdis.nasa.gov/firemap/>). The fires started on 7 June 2013, close to the south-west coast of Hudson Bay. By 27 June, a road of fire had formed from Alaska to Labrador, via Lake Athabaska, the area around the southern end of Hudson Bay and James Bay, first somewhat patchy then maximizing in early July (Fig. 1). The fires diminished significantly after 12 July.

Also in the USA a changing number of fires burnt. They were located more in the southern half of the country, but in early July large areas in the west and south of the Great Lakes were covered with fires. In addition, many fires burnt also in Siberia during that period (not shown).

OMI aerosol maps show quite a few spectacular fire events along this road of fire. An extreme phase with the aerosol index even reaching the scale limit was 1–7 July (Fig. 2), coinciding with the phase of maximum fire activity identified from the FIRMS images. In this phase very likely



**Table 1.** List of the lidar sounding days at IMK-IFU and UFS (Garmisch-Partenkirchen, Germany) during the smoke period in July 2013; min means the minimum altitude of observation (1000–1200 m a.s.l.), P, S, M, K, G the radiosonde stations Payerne, Stuttgart, Munich, Kümmersbruck, and Graz, respectively. The sonde stations were selected based on the trajectory results. Maximum backscatter coefficients in brackets could be due to clouds. Sonde RH is listed only if significantly below 10%. Typical peak ozone values are printed in italics, layer positions for DIAL measurements in bold.

Date	Aerosol Ranges (km)	Max. $\beta$ ( $10^{-6} \text{ m}^{-1} \text{ sr}^{-1}$ )	Elevated $\text{O}_3$ (km)	Low $\text{H}_2\text{O}$ in range (km)
1 July	min–5.5 7.0–12.5	2.0 0.3	3.6–5.7 8.5–11.0 <i>(80–100 ppb)</i>	4–4.5, 5.2, 5.8–6.5 7–7.6 (P, 00:00 UTC)
2 July	min–5.2 5.5–8.2	5.3 1 (5.2)	3.3–5.6 <i>(75 ppb)</i>	around 4 km (P, 00:00 UTC)
8 July	min–5.8, E. Europe	9.6	4.8–8	
9 July	min–2.6, E. Europe 2.6–4.9, E. Europe	5.1 1.7	3.5–9	
11 July	min–3.5 3.7–6.4	21 (40.5) 2.8	1.4–3.5 3.7–8 <i>(65–80 ppb)</i>	layers 3–7 (S) layers 3–7 (S)
12 July	min–3.4 3.6–6.1 6.1–10.6	5.8 19.8 1.2	3.1–5.0 5.0–10.5 <i>both (90–100 ppb)</i>	3.4–4.8 (S, 00:00 UTC)
13 July	min–3.5 4.5–11	3.6 6.1	1.5–3.3 3.6–8.8	2.3–2.7 (S, 00:00 UTC)
15 July	min–3.6 3.6–6.7	5 10.3 (44)	3–5 5.7–10.5	3.6–3.7 (S, 00:00 UTC) M missing
16 July	min–6.2	11.8	3.2, 4.5 <i>(80–85 ppb)</i>	<b>3.2, 4.5 (DIAL)</b>
18 July	min–5.9	15 (76)	<i>excursion <math>\leq 5 \text{ ppb}</math></i>	<b>3.2 (DIAL)</b>
19 July	1.1–4.7	4.8	2–4 <i>(70–75 ppb)</i>	3.7 (G, 18 July, 03:00 UTC)
22 July	min–3 3–4	4.6 (7.3) 0.9	4.3–5.2 <i>(75 ppb)</i>	3.1–5.3 (K)
23 July	min–3.3 3.3–4.9	2.9 2.0		<b>3.2, 4.1 (DIAL)</b>
25 July	min–5	most likely Saharan dust		

specific broad hump during the smoke period in July. This hump is accompanied by a similar hump in CO, reaching roughly 125 ppb around 15 July, that is not present during the second half of June and by the end of July when advection of Saharan dust prevailed (particle sizes between 1 and 7  $\mu\text{m}$ ). This suggests at least some descent of the polluted air from Canada to the altitude range below 3 km. The lidar results give evidence of a pronounced smoke layer around 3 km only on 3 days.

## 4.2 Lidar examples

An overview of the lidar measurements at Garmisch-Partenkirchen during the smoke period in July 2013 is given in Table 1. We give the range of aerosol layers, maximum backscatter coefficients, elevated free-tropospheric ozone, as

well as dry layers (also confirmed by trajectory calculations as done in the four examples presented below). On 8 and 9 July advection from the east took place and no sign of smoke import from North America was found. Elevated aerosol in both the lidar and the ceilometer measurements (including Leutkirch) during that period are more likely due to widely spread fires north of the Black Sea and in Russia. On 25 July a transition to a new Saharan dust period started.

In the following we present the data for 4 selected days that demonstrate the considerable variability of the vertical distribution of the smoke layers. With the exception of 16 July just brief interpretations are given.



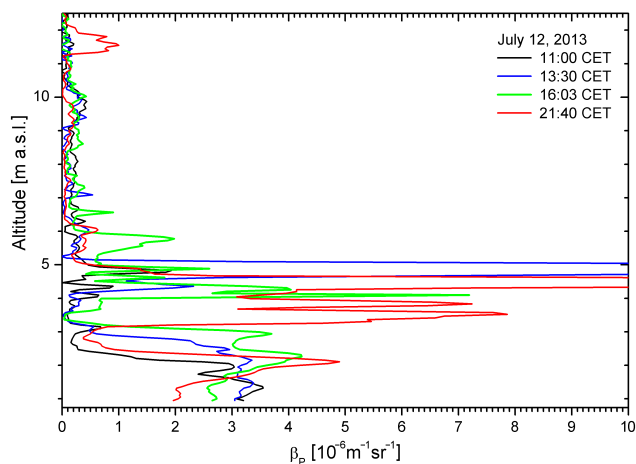


**Figure 8.** 313 nm particle backscatter coefficients selected from the profiles of 12 July 2013. The peak value is given in the text.

#### 4.2.1 2 July 2013

The first 2013 observation of small amounts of smoke above Garmisch-Partenkirchen was made on 1 July 2013. On 2 July pronounced structures appeared. After a frontal passage with a thunderstorm during the second half of the night advection from the Atlantic started, clearing until 08:00 CET (central European time; CET = UTC + 1 h). Figures 5 and 6 show the 313 nm aerosol backscatter coefficients and the corresponding ozone mixing ratios, respectively. The distribution of ozone shows moderate values for this season (50 ppb) within the ranges of enhanced aerosol (5.5–8 km) but up to 75 ppb in the initially aerosol-free intermediate range between 3.5 and 5.0 km. The H<sub>2</sub>O lidar was not available on that day and we, instead, examined radiosonde data. Westerly advection prevailed in that vertical range and, as a consequence, Payerne was the most adequate radiosonde station in this. Between 00:00 and 12:00 UTC the Payerne RH near 4 km dropped from 12 to 6%. Elevated ozone plus low RH could suggest the presence of some stratospheric air component.

The daily stratospheric-intrusion forecasts (Zanis et al., 2003; Trickl et al., 2010, 2014) that identify these descending layers based on potential vorticity were not available for most of July 2013. Thus, we used HYSPLIT backward trajectory calculations. For the layer between 3.5 and 5 km, HYSPLIT (09:00 UTC = 10:00 CET) indicated some air components descending from roughly 7 km above the ground over Canada (at –315 h), slightly north of the Great Lakes, with some tendency for rising towards earlier times. This confirms the idea of a stratospheric component in that air mass. There was no aerosol between 3.9 and 5.0 km in the morning, indicative of potential ozone formation in a fire plume.

In Fig. 7, three HYSPLIT backward trajectories initiated in the aerosol layer between 5.5 and 8 km at 11:00 CET are displayed. The air mass travelled in the middle and upper troposphere, over Canada mostly clearly north of the fire zone

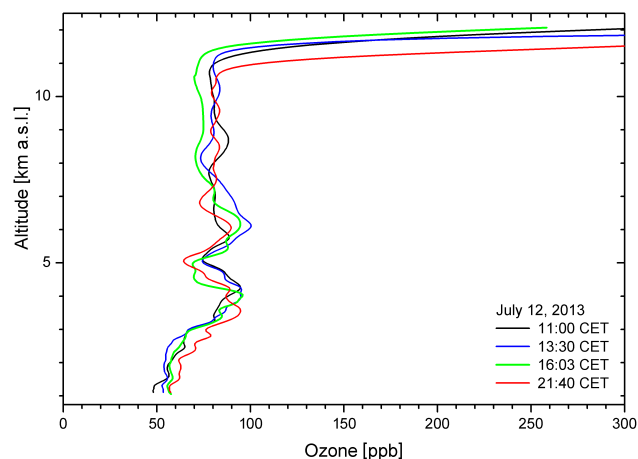


**Figure 9.** Ozone profiles selected from the results of 12 July 2013, and corresponding to the cases shown in Fig. 5; please note that the upper-tropospheric uncertainty is of the order of 10 ppb due to the radiation loss caused by the high, lower- and mid-tropospheric ozone densities and the aerosol layers.

of Fig. 1. For most of the trajectories just over Alaska or the Northwest Territories an overlap with the fires reported there could have occurred. A few trajectories for slightly different start times or altitudes (not shown) pass over the north-western part of the USA but before the onset of the fire period there. However, the 6300 m trajectory in Fig. 7 hits a strong fire plume over the central Québec province revealed by the OMI images around 29 June. Unless there is an influence from Siberia, this fire is the most probable explanation for our observations on 2 July. The pattern of Fig. 7 was confirmed by HYSPLIT ensemble trajectories.

The O<sub>3</sub> mixing ratios of about 50 ppb in that layer are low for this part of the year and are, thus, not indicative of pronounced ozone production within this fire plume.

Trajectories initiated within the lower aerosol layer passed eastern France and the United Kingdom at more than 1.5 km above the ground and reach the boundary layer above the Atlantic between Iceland and the Canadian coast for backward times up to the maximum of 315 h. No attempt of an interpretation is made.

#### 4.2.2 12 July 2013

The measurements on 12 July 2013 (Figs. 8, 9) show the presence of smoke plumes up to 7.1 km, the most pronounced structures having been limited to altitudes up to about 5 km. The peak backscatter coefficient (13:00 CET) reached  $2.0 \times 10^{-5} \text{ m}^{-1} \text{ sr}^{-1}$  (13:00 CET), corresponding to a very low horizontal standard visual range of just about 4 km.

The optically thickest layers travelled below 6 km. Two layers of elevated ozone persisted around 4 and 6 km. For most of the day the main part of the smoke stayed above

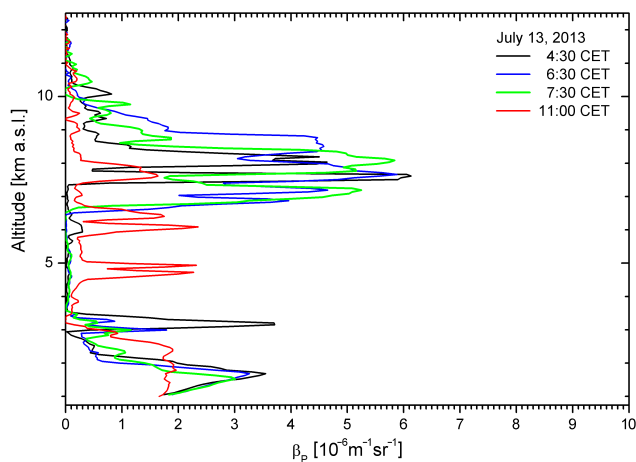


**Figure 10.** 313 nm particle backscatter coefficients for 13 July 2013; on this day almost the entire troposphere was filled with aerosol layers from the Canadian fires.

4 km. However, at 21:40 CET a lot of aerosol was also found in the lower-lying high-ozone layer. The trajectory analyses for this layer in the morning yield strong subsidence from Greenland and the Canadian polar islands but with altitudes not exceeding 7 km. Nevertheless, the radiosonde station relevant for the direction of air-mass arrival, Stuttgart, shows minimum RH values of 3 % for both 00:00 and 12:00 UTC between 3 and 4 km, confirming the idea of a stratospheric intrusion. In the afternoon, import from the fire zone in Canada is verified but with some indicated subsidence from beyond North America towards 315 h backward in time. The Stuttgart RH for 24:00 UTC is, still, 4–6 % around 2.6 km.

The upper ozone peak at around 6 km is most pronounced in the afternoon. This agrees with the trajectory analysis that indicates growing stratospheric influence during the second half of the day.

#### 4.2.3 13 July 2013

High levels of aerosol were observed in discrete layers throughout the troposphere on 13 July 2013, in the early morning mostly in the upper troposphere (Fig. 10). This upper tropospheric air mass was verified having descended from the region around the fires.

At 04:30 CET the aerosol peak at 3.2 km coincides with a stratospheric intrusion layer (Fig. 11) anti-cyclonically descending from about 8 km above the Canadian polar islands and Greenland via Norway. It is interesting to note the maximum altitude within 315 h is found by HYSPLIT at exactly 3.2 km a.s.l. over our site, but locates the import from the zone of fires when initializing the trajectories 0.2–0.3 km above this. The midnight sonde data for Payerne, Stuttgart, and Munich show minimum RH values of 3–6 %, a few hundred metres lower, in agreement with the expectations of the trajectories.

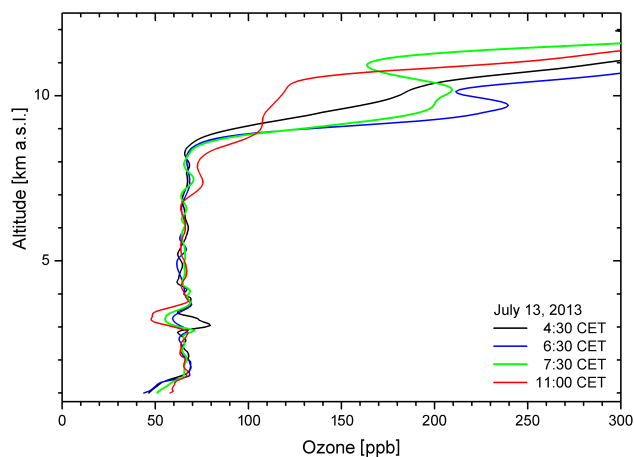


**Figure 11.** Ozone profiles for 13 July 2013, the upper-tropospheric uncertainty is of the order of 10 ppb due to the radiation loss caused by the high densities and the aerosol layers.



**Figure 12.** View from the Zugspitze summit approximately to the south on 16 July 2013, at 09:00 CET; the Canadian fire plume fully hits the summit, but the main part misses Hohe Munde (2662 m a.s.l., to the left, distance 10.6 km). At the horizon, to the right, the summits of the central Alps, reaching 3774 m a.s.l. (Wildspitze, Austria), appear just above the smoke layer (difficult to discern without magnification). The Schneefernerhaus station is slightly outside the picture (to the right). Source: <http://zugspitze.panamax.at> (copyrighted), courtesy of *visualisierung und informationstechnologie* (Austria).

During the following hours both the aerosols at this altitude and ozone drop considerably. At 11:00 CET a 50 ppb “ozone hole” was registered between 3.2 and 3.4 km (Fig. 11). HYSPLIT confirms travel altitudes below the stratosphere, but due to a lot of different continental (USA, Canada) and marine source regions the interpretation is difficult. The complete absence of smoke around 3.2 km cannot be explained.

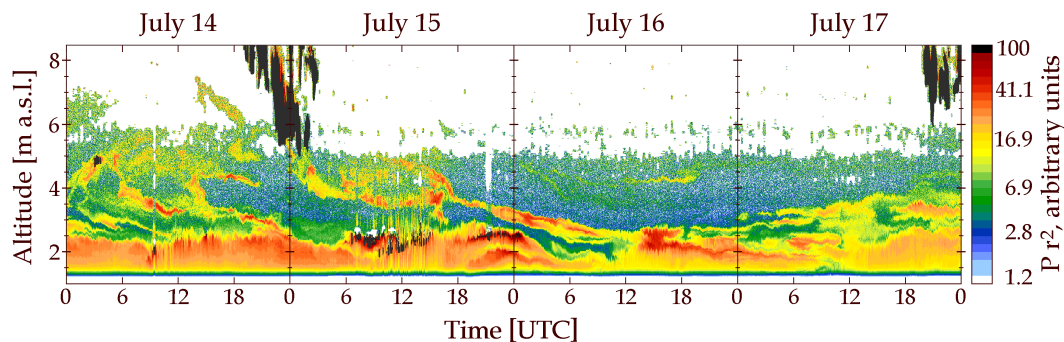


**Figure 13.** Range-corrected backscatter signal ( $P(r)r^2$ ; logarithmic colour code) measured by ceilometer over Hohenpeißenberg (southern Germany) from 14 to 17 July 2013. Areas with low signal-to-noise ratio are masked white. On 16 July, the smoke layer descended to an altitude below that of the Zugspitze summit until noon, followed by a slight rise in the afternoon.

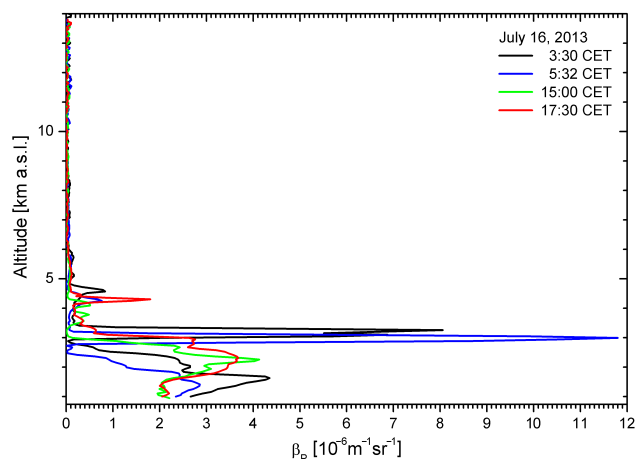


**Figure 14.** 313 nm particle backscatter coefficients for 16 July 2013; the peak backscatter coefficient at 05:32 CET,  $1.2 \times 10^{-5}$ , corresponds to a horizontal standard visual range of the order of 6.5 km.

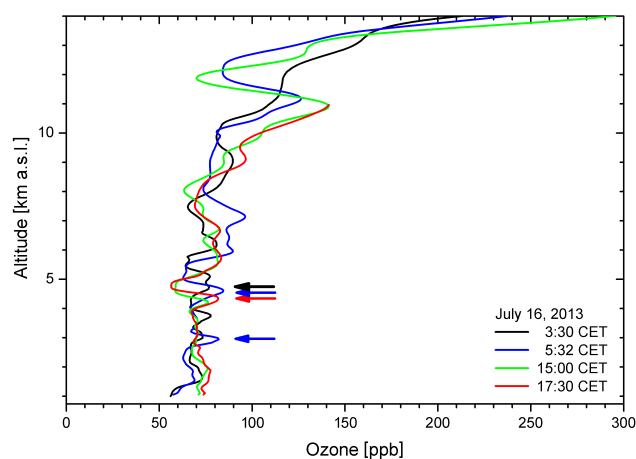


**Figure 15.** Ozone profiles for 16 July 2013. In the layers of strongly enhanced aerosol below 5 km the ozone mixing ratio is several times slightly elevated (see arrows, colour chosen as in corresponding curves). Elevated ozone is seen also in other layers.

The 12:00 UTC radiosonde ascents at both Stuttgart and Payerne show RH values of the order of 50 % at around 3.3 km, which is not extremely humid but indicative of PBL air.

In the upper troposphere there is no obvious positive correlation between the fire particles and ozone, with some uncertainty given by the aerosol correction and vertical averaging over rather large intervals. The Stuttgart and Munich radiosonde RH values above 3 km are above any expectations for stratospheric air, supporting these results.

#### 4.2.4 16 July 2013

A particularly interesting situation occurred on 16 July 2013 because a particularly dense and thin smoke plume directly hit the Zugspitze summit (2962 m a.s.l.). The plume was not clearly visible from the valley, but the sky turned suddenly dark when the Zugspitze cable car approached the top sta-

tion. An example is given in Fig. 12, showing a southward section of the 360° image of the Zugspitze web camera. From the high summits below and above the plume one can estimate the extent of that layer at just several hundred metres. The Schneefernerhaus research station (UFS, not visible in Fig. 12) on the south face of the Zugspitze (lidar laboratory: 2675 m) is located at the lower edge of the plume as one can judge from the approximately equally high mountain Hohe Munde (2662 m a.s.l.) to the left. Since we look at that summit from inside the plume we estimate a horizontal standard visual range of less than 10 km. To the west and north-west (not shown) the colour of the smoke layer was even almost completely dark, indicating the presence of soot particles.

In Fig. 13, a 4-day section of the Hohenpeißenberg ceilometer measurements including 16 July is displayed. In agreement with the slightly anti-cyclonic situation, subsidence is observed. The smoke layers descended similarly to stratospheric intrusion layers frequently mapped with the

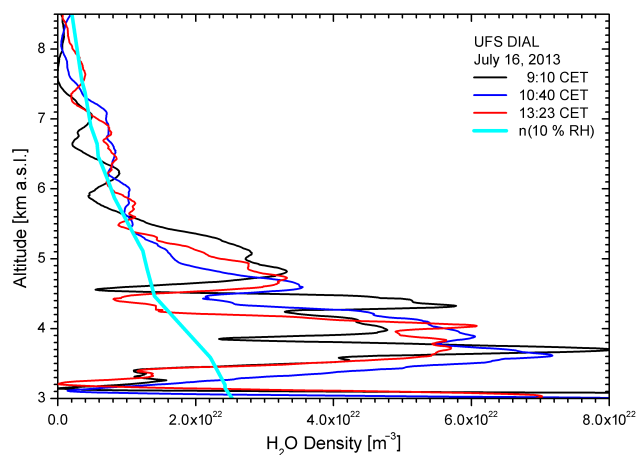


**Figure 16.** Water-vapour profiles obtained with the UFS DIAL on 16 July 2013 together with the 10 % RH curve from the Stuttgart radiosonde (Munich data not being available); the layer with most aerosol is extremely dry suggesting the presence of stratospheric air. Also in the aerosol layer around 4.5 km relative humidity values of the order of just 5 % are seen indicating a strong stratospheric component.

IFU lidar systems, suggesting a similar layer topography. There is no evidence that the smoke penetrated into the boundary layer in the afternoon of 16 July. As in the case of many observations of stratospheric intrusions with the ozone DIAL, the layer seems to slide primarily along the top of the boundary layer.

The UFS ceilometer confirms the absence of subsidence below the Schneefernerhaus and suggests just partial overlap of the aerosol layer with the station after roughly 08:00 CET (not shown). The upper edge stayed at about 3.3 km until noon and slightly rose in the afternoon. The reason of the difference with respect to the Hohenpeißenberg measurement is ascribed to orographic lifting above the high mountain. We have routinely also observed differences of layer altitudes between the ozone DIAL and the Zugspitze summit station.

Due to an excursion to UFS the measurements with the ozone DIAL were only made in the early morning and in the late afternoon. The thin smoke layer and additional aerosol spikes are clearly visible in 313 nm backscatter coefficients (Fig. 14). The maximum backscatter coefficient was  $1.2 \times 10^{-5} \text{ m}^{-1} \text{ sr}^{-1}$ , corresponding to a 313 nm horizontal standard visual range of about 6.5 km, in agreement with the visual observations (Fig. 12). Within the plumes slightly elevated ozone is visible (Fig. 15). It is important to note that the uncertainty due the aerosol correction is clearly smaller than the size of the  $\text{O}_3$  peak in the ozone profile.

The nature of the elevated ozone in the smoke layers was revealed by the humidity measurements. The first day in July 2013 when the water-vapour DIAL was operated was 16 July. The results are displayed in Fig. 16 and show low humidity within the two partial plumes at about 3.2 and 4.5 km.

The extremely low water-vapour density in the main layer clearly verifies the presence of stratospheric air. The average minimum density,  $8.8 \times 10^{20} \text{ m}^{-3}$  ( $\pm 1.1 \times 10^{21} \text{ m}^{-3}$ ), corresponds to a mixing ratio of 48 ppm and 0.36 % RH. This result corresponds to values typically found in intrusions, as published by Trickl et al. (2014), but is puzzling since the dense smoke in the layer suggests mixing with tropospheric air. In the range of the upper aerosol layer (varying in altitude between 4.2 and 4.7 km) the minimum water-vapour density is  $5.4 \times 10^{21} \text{ m}^{-3}$  (4.2 % RH), i.e., in better agreement with the idea of mixing.

On 2 additional days, 18 and 23 July, DIAL measurements of water vapour were made. The minimum  $\text{H}_2\text{O}$  densities within the plume are of the order of  $2 \times 10^{22} \text{ m}^{-3}$ , which is dry but far away from unperturbed layers of stratospheric origin. The minimum relative humidity values on the other days (Table 1) have been imported from radiosonde data and are below 10 % whenever dry layers exist.

The dry layer at 3.2 km on 16 July becomes even more amazing when calculating HYSPLIT backward trajectories. We calculated trajectories every 100 m for altitudes between 3000 and 3600 m a.s.l. over Garmisch-Partenkirchen because of the issues in the HYSPLIT orography mentioned before. The highest backward altitudes, i.e., those reflecting the highest probability of STT, were obtained for start altitudes around 3500 m. The trajectories of at least 3400 m remain in a highly confined bundle all the way back to the west coast of Canada, in the vicinity of Vancouver, and reveal almost steady air-mass subsidence. One example is given in Fig. 17. A pronounced coherence was also found by calculating HYSPLIT “ensemble” trajectories.

At 13 days backward in time, the altitudes still remained at 7 km or less, i.e., somewhat below the typical stratospheric values for this time of the year. Therefore, we calculated extension trajectories for the bundle starting above our site at 3500 m a.s.l., which initiated over the southern end of James Bay where the initial trajectory bundle was, still, highly confined. We found a continued backward rise: another 2–6 days backward in time, altitudes of 7.5–9 km were reached above Siberia and the Arctic Ocean (Fig. 18). This backward rise towards Asia is a general feature here, not highly dependent on the start conditions, although the source regions change. However, the degree of coherence presented considerably surpasses any behaviour seen in many years of HYSPLIT calculations for classifying our observations. In our 2011 study (Trickl et al., 2011) we found similarly coherent air streams with FLEXPART but not over that many days.

It is interesting to note that a forward trajectory triplet calculated for the start coordinates of the extension trajectories in Fig. 18 passes over southern Bavaria less than 100 km from Garmisch-Partenkirchen, and two of the three trajectories crossing the northern rim of the Alps pass even much closer.

The trajectory results qualitatively agree with the general flow exhibited in the satellite images. Most importantly,

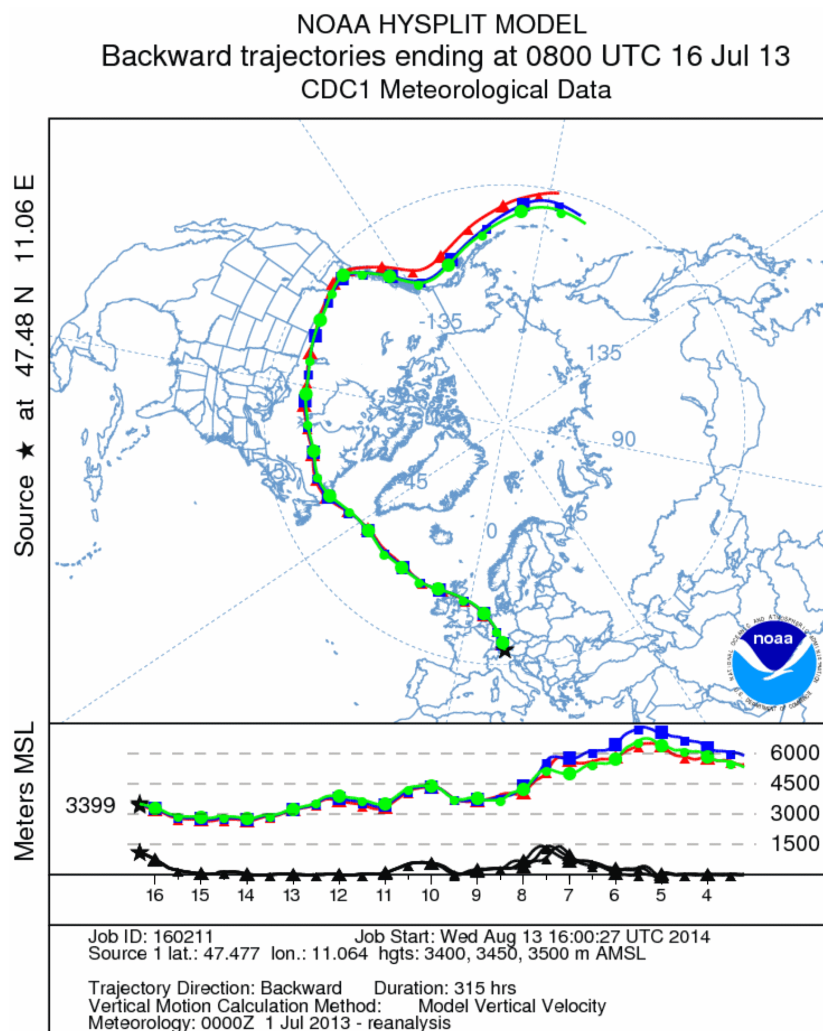


**Figure 17.** HYSPLIT backward trajectories calculated for altitudes of 3400, 3500 and 3600 m a.s.l. over Garmisch-Partenkirchen showing almost steady subsidence from the North Pacific within 315 h. AMSL: above mean sea level. The black line in the altitude box shows the ground level.

we were able to find two aerosol layers over the Québec province at 3.0 and 4.2 km in the CALIOP image for 9 July, 06:41–06:55 UTC, which strongly supports our analysis. The aerosol was followed with CALIOP images all the way across the Atlantic but with less perfect temporal matching.

Although these trajectories look robust and extremely coherent, trajectory analyses certainly have limitations. Without the measurements of the water-vapour DIAL this kind of analysis would be somewhat uncertain. A descent of an extremely dry layer over more than 15 days exceeds even the 13-day range of analysis in our recent paper (Trickl et al., 2014).

Despite the location of UFS just at the lower edge of the smoke layer, there are clear signs in the data registered there (Fig. 19). After 09:00 CET a slight simultaneous increase of  $O_3$ , CO,  $PM_{10}$  and the condensation nuclei is visible. The in-

crease in ozone by about 8 ppb supports the lidar results. In contrast to the visual impression at the summit, black carbon did not rise as rapidly as the other species. Since the aerosol instrumentation at the summit station was not running, no measurement directly inside the smoke plume is available. The summit RH clearly shows the dry conditions during the intrusion period (Fig. 19), but the minimum value is significantly higher than expected from the lidar measurements. This is nothing new (Trickl et al., 2014), but, on the other hand, the intrusion hit the summit before the first  $H_2O$  measurement with the DIAL system. Thus, no direct comparison is possible. Finally, the rise in the in situ ozone qualitatively confirms the lidar results (Fig. 15), but was less pronounced due to the partial overlap of UFS with the layer.

Also the RH data for UFS (not shown) show values of 25 % and less in the morning with just a 2 h delay with re-

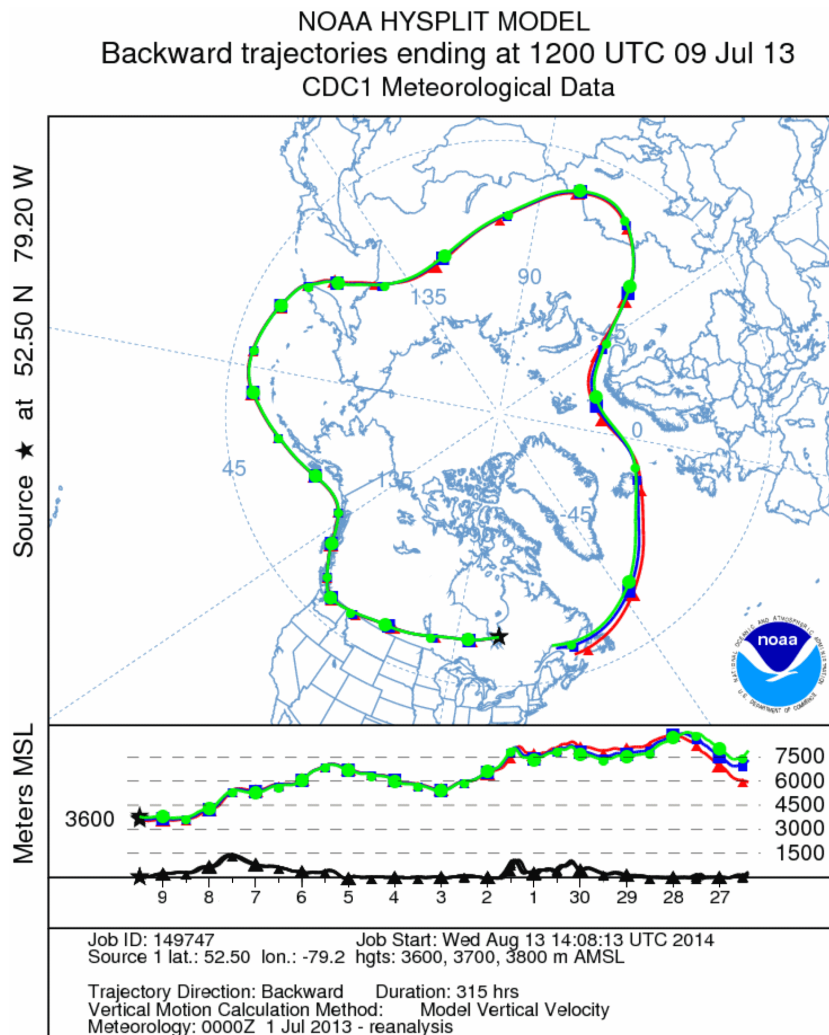


**Figure 18.** Extension backward trajectories for those in Fig. 17 initiated on 9 July 2013 (12:00 UTC) at altitudes of 3600, 3700 and 3800 m a.s.l. over James Bay where the three trajectories in Fig. 17 almost coincide. The coherence of the trajectory bundle is exceptional. The maximum altitude reached is about 9 km.

spect to the summit. This also demonstrates the partial overlap with the intrusion layer. The rise in ozone and aerosol occurred in the second half of the dry period, the time agreeing with the end of the subsidence revealed by the ceilometer data for UFS. The H<sub>2</sub>O measurements with the DIAL confirm the slight lifting of the layer starting around noon, explaining the end of the highest ozone and aerosol values in the in situ data.

## 5 Discussion and conclusions

Our results for July 2013 have revealed a number of details on the long-lasting boreal fire plumes from North America. There are both aerosol layers with moderate and enhanced ozone mixing ratios. The analysis shows that elevated ozone was strongly related to the presence of stratospheric air for

the cases examined. As can be seen from Table 1, dry layers were observed on all 11 measurement days on which smoke import from Canada or Alaska was verified. We conclude that ozone production as claimed for boreal fire plumes reaching lower latitudes (e.g., Wotawa and Trainer, 2000; Real et al., 2007; Val Martin et al., 2006) cannot be strong.

This is nothing surprising. For instance, Jacob et al. (1992) found very low O<sub>3</sub> formation in Alaska fire plumes. They concluded that ozone build-up was limited to the first day of travel when NO<sub>x</sub> concentrations were relatively high. Alvarado et al. (2010) also conclude on little evidence of O<sub>3</sub> formation downwind high-latitude fires as a consequence of efficient conversion of NO<sub>x</sub> to PAN. Ozone formation in dense smoke is also reduced due to the absorption of solar radiation (e.g., Verma et al., 2009).

The role of descending stratospheric air masses for the ozone budget over boreal North America has been dis-

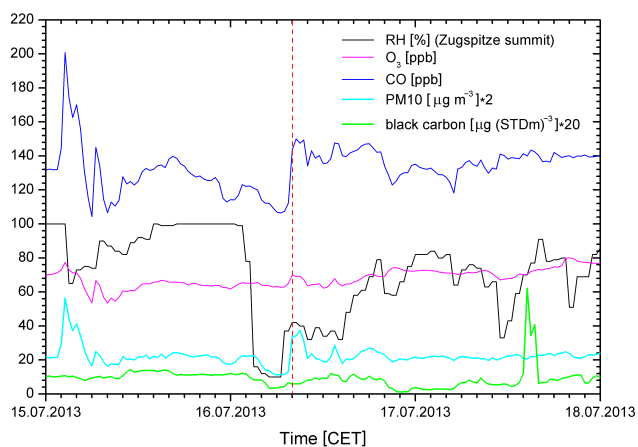


**Figure 19.** Selected measurements at UFS between 15 and 17 July 2013. The dashed vertical line (09:00 CET) marks the arrival of the edge of the smoke layer at the station. The relative-humidity data are taken from the listings of the German Weather Service (DWD) at the Zugspitze summit located 0.3 km higher than UFS. The dry smoke layer was observed earlier there.

cussed before (e.g., Wofsy et al., 1992; Gregory et al., 1992; Mauzerall et al., 1996). Our results for July 2013 (and at a lower smoke level for summer 2014) examples indicate that long-range transport of smoke from boreal fires from North America or eastern Siberia to Europe in stratospheric intrusion layers could be a rather important transport mechanism. Relevant are the so-called Type-6 intrusions defined by Trickl et al. (2010). These intrusions frequently exhibit a gradual descent from Siberia, Alaska and western Canada to Europe over 1–2 weeks, thus contrasting the rapid descent of the well-known intrusions from Greenland and its surroundings (mostly Types 1 and 2). They can be observed at the high-lying Alpine stations and add-up together with the Type-5 intrusions from eastern Canada to about one-third of the intrusions during the summer intrusion minimum. Our measurements show that they are even more frequent if one includes higher altitudes, an important result of our recent routine measurements.

The age spectra generated with FLEXPART model calculations for the stations Mt. Cimone, Zugspitze, Sonnblick and Jungfraujoch suggest that long transport times even dominate the stratospheric contributions (Stohl et al., 2000; Trickl et al., 2010) at these sites. At higher altitudes the summer minimum diminishes (e.g., Beekmann et al., 1997), in agreement with the high number of stratospheric layers in our lidar data throughout the year.

The observation of smoke travelling in intrusion layers is interesting and particularly puzzling in the case of 16 July. It is not possible to determine how the smoke got trapped in the layer at 3.2 km without significantly modifying the humidity and the layer because there are no detailed observations in the source region. The air ascending in the fire was

most likely very dry since the formation of wildfires requires rather dry conditions. Stirring of the stratospheric layer by a strongly ascending hot air mass does not look like a good solution. Therefore, we prefer the idea that the stratospheric air tongue intersected a smoke column in a later, more stationary phase. There is also the possibility of sedimentation of heavy particles from a layer crossing above, but this looks rather complex and is not discussed further here.

The example of 16 July impressively confirms our recent study (Trickl et al., 2014) that dry layers descending from the lower stratosphere can survive almost unchanged for as much as 13 days, here very likely even for several more days. The intrusions slowly descended over extremely long distances (Type 6 as defined by Trickl et al., 2010) contrasting the typical direct Type-1 and Type-2 intrusions from Greenland to central Europe.

In summary, the observations in July 2013 confirm our idea of direct transport from boreal North America to Europe in subsiding air masses without strong loss of particle density. A rather stable weather pattern allowed for the inflow of smoke over a period of several weeks, interrupted on just 2 days.

*Acknowledgements.* The authors from IMK-IFU thank H. P. Schmid for his interest and support. We thank the UFS team for their great assistance. The aerosol instrumentation operated by UBA and its quality assurance benefit from a co-operation with the Leibnitz Institute for Tropospheric Research. The IFU aerosol results contribute to the European Aerosol Research Lidar Network (EARLINET) that is currently partly funded within the European project ACTRIS. The development of the water-vapour DIAL and the early measurements with this system were funded by the Bavarian Ministry of Economics and German Federal Ministry of Education and Research within the programme Atmosphärenforschung 2000 (ATMOFAST, 2005).

The article processing charges for this open-access publication were covered by a Research Centre of the Helmholtz Association.

Edited by: J. Roberts

## References

- Alvarado, M. J., Logan, J. A., Mao, J., Apel, E., Riemer, D., Blake, D., Cohen, R. C., Min, K.-E., Perring, A. E., Browne, E. C., Wooldridge, P. J., Diskin, G. S., Sachse, G. W., Fuelberg, H., Sessions, W. R., Harrigan, D. L., Huey, G., Liao, J., Case-Hanks, A., Jimenez, J. L., Cubison, M. J., Vay, S. A., Weinheimer, A. J., Knapp, D. J., Montzka, D. D., Flocke, F. M., Pollack, I. B., Wennberg, P. O., Kurten, A., Crouse, J., Clair, J. M. St., Wisthaler, A., Mikoviny, T., Yantosca, R. M., Carouge, C. C., and Le Sager, P.: Nitrogen oxides and PAN in plumes from boreal fires during ARCTAS-B and their impact on ozone: an integrated analysis of aircraft and satellite observations, *Atmos. Chem. Phys.*, 10, 9739–9760, doi:10.5194/acp-10-9739-2010, 2010.
- Amiridis, V., Balis, D. S., Kazadzis, S. Bais, A., Giannakaki, Pappayannis, A., and Zerefos, C.: Four-year aerosol observations with a Raman lidar at Thessaloniki, Greece, in the framework of European Aerosol Research Lidar Network (EARLINET), *J. Geophys. Res.*, 110, D21203, doi:10.1029/2005JD006190, 12 pp., 2005.
- ATMOFAST: Atmosphärischer Ferntransport und seine Auswirkungen auf die Spurengaskonzentrationen in der freien Troposphäre über Mitteleuropa (Atmospheric Long-range Transport and its Impact on the Trace-gas Composition of the Free Troposphere over Central Europe), Project Final Report, Co-ordinator: Trickl, T., subproject Co-ordinators: Kerschgens, M., Stohl, A., and Trickl, T., funded by the German Ministry of Education and Research within the programme “Atmosphärenforschung 2000”, 130 pp., available at: <http://www.trickl.de/ATMOFAST.htm> (last access: 26 August 2015), 2005 (in German; revised publication list 2012).
- Beekmann, M., Ancellet, G., Blonsky, S., De Muer, D., Ebel, A., Elbern, H., Hendricks, J., Kowol, J., Mancier, C., Sladkovic, R., Smit, H. G. J., Speth, P., Trickl, T., and Van Haver, P.: Regional and Global Tropopause Fold Occurrence and Related Ozone Flux across the Tropopause, *J. Atmos. Chem.*, 28, 29–44, 1997.
- Birmili, W., Göbel, T., Sonntag, A., Ries, L., Sohmer, R., Gilge, S., Levin, I., and Stohl, A.: A case of transatlantic aerosol transport detected at the Schneefernerhaus Observatory (2650 m) on the northern edge of the Alps, *Meteorol. Z.*, 19, 591–600, 2010.
- Bösenberg, J., De Tomasi, F., Eixmann, R., Freudenthaler, V., Giehl, H., Grigorov, I., Hågård, A., Iarlori, M., Kirsche, A., Kolarov, G., Komguem, L., Kreipl, S., Kumpf, W., Larchevêque, G., Linné, H., Matthey, R., Mattis, I., Mekler, A., Mironova, I., Mitev, V., Mona, L., Müller, D., Music, S., Nickovic, S., Pandolfi, M., Pappayannis, A., Pappalardo, G., Pelon, J., Pérez, C., Perrone, R. M., Persson, R., Resendes, D. P., Rizi, V., Rocadenbosch, F., Rodrigues, J. A., Sauvage, L., Schneidenbach, L., Schumacher, R., Sherbakov, V., Simeonov, V., Sobolewski, P., Spinelli, N., Stachlewska, I., Stoyanov, D., Trickl, T., Tsaknakis, G., Vaughan, G., Wandinger, U., Wang, X., Wiegner, M., Zavrtnik, M., and Zerefos, C.: EARLINET: A European Aerosol Research Lidar Network to Establish an Aerosol Climatology, Co-ordinator: Bösenberg, J., Max-Planck-Institut für Meteorologie (Hamburg, Germany), Report No. 348, ISSN 0937 1060, 155 pp., 2003.
- Brioude, J., Cooper, O. R., Trainer, M., Ryerson, T. B., Holloway, J. S., Baynard, T., Peischl, J., Warneke, C., Neuman, J. A., De Gouw, J., Stohl, A., Eckhardt, S., Frost, G. J., McKeen, S. A., Hsie, E.-Y., Fehsenfeld, F. C., and Nédélec, P.: Mixing between a stratospheric intrusion and a biomass burning plume, *Atmos. Chem. Phys.*, 7, 4229–4235, doi:10.5194/acp-7-4229-2007, 2007.
- Browell, E. V., Gregory, G. L., Harriss, R. C., and Kirchoff, V. W. J. H.: Tropospheric Ozone and Aerosol Distributions Across the Amazon Basin, *J. Geophys. Res.*, 93, 1431–1451, 1988.
- Carnuth, W. and Trickl, T.: Transport studies with the IFU three-wavelength aerosol lidar during the VOTALP Mesolcina experiment, *Atmos. Environ.*, 34, 1425–1434, 2000.
- Carnuth, W., Kempfer, U., and Trickl, T.: Highlights of the Tropospheric Lidar Studies at IFU within the TOR Project, *Tellus B*, 54, 163–185, 2002.
- Crutzen, P. J. and Andreae, M. O.: Biomass Burning in the Tropics: Impact on Atmospheric Chemistry and Biogeochemical Cycles, *Science*, 250, 1669–1678, 1990.
- Cui, J., Pandey Deolal, S., Sprenger, M., Henne, S., Staehelin, J., Steinbacher, M., and Nédélec, P.: Free tropospheric ozone changes over Europe as observed at Jungfraujoch (1990–2008): An analysis based on backward trajectories, *J. Geophys. Res.*, 116, D10304, doi:10.1029/2010JD015154, 2011.
- Damoah, R., Spichtinger, N., Forster, C., James, P., Mattis, I., Wandinger, U., Beirle, S., Wagner, T., and Stohl, A.: Around the world in 17 days – hemispheric-scale transport of forest fire smoke from Russia in May 2003, *Atmos. Chem. Phys.*, 4, 1311–1321, doi:10.5194/acp-4-1311-2004, 2004.
- Delany, A. C., Haagensen, P., Walters, S., Wartburg, A. F., and Crutzen, P. J.: Photochemically Produced Ozone in the Emissions From Large-Scale Tropical Vegetation Fires, *J. Geophys. Res.*, 90, 2425–2429, 1985.
- Draxler, R. and Hess, G.: An overview of the HYSPLIT\_4 modelling system for trajectories, dispersion, and deposition, *Aust. Meteorol. Mag.*, 47, 295–308, 1998.
- Eisele, H. and Trickl, T.: Second Generation of the IFU Stationary Tropospheric Ozone Lidar, in: *Advances in Atmospheric Remote Sensing with Lidar, Selected Papers of the 18th International Laser Radar Conference, Berlin (Germany), 22–26 July 1996*, edited by: Ansmann, A., Neuber, R., Rairoux, P., Wandinger, U., pp. 379–382, Springer (Berlin, Heidelberg, Germany), 1997.
- Eisele, H. and Trickl, T.: Improvements of the aerosol algorithm in ozone-lidar data processing by use of evolutionary strategies, *Appl. Optics*, 44, 2638–2651, 2005.
- Eisele, H., Scheel, H. E., Sladkovic, R., and Trickl, T.: High-resolution Lidar Measurements of Stratosphere-troposphere Exchange, *J. Atmos. Sci.*, 56, 319–330, 1999.
- Fehsenfeld, F. C., Ancellet, G., Bates, T. S., Goldstein, A. H., Hardesty, R. M., Honrath, R., Law, K. S., Lewis, A. C., Leitch, R., McKeen, S., Meagher, J., Parrish, D. D., Pszenny, A. A. P., Russell, P. B., Schlager, H., Seinfeld, J., Talbot, R., and Zbinden, R.: International Consortium for Atmospheric Research on Transport and Transformation (ICARTT): North America to Europe – Overview of the 2004 summer field study, *J. Geophys. Res.*, 111, D23S01, doi:10.1029/2006JD007829, 2006.
- Fishman, J. and Larsen, J. C.: Distribution of Total Ozone and Stratospheric Ozone in the Tropics: Implications for the Distribution of Tropospheric Ozone, *J. Geophys. Res.*, 92, 6627–6634, 1987.
- Fishman, J., Minnis, P., and Reichle, H. G.: Use of Satellite Data to Study Tropospheric Ozone in the Tropics, *J. Geophys. Res.*, 91, 14451–14465, 1986.



- Flentje, H., Claude, H., Elste, T., Gilge, S., Köhler, U., Plass-Dülmer, C., Steinbrecht, W., Thomas, W., Werner, A., and Fricke, W.: The Eyjafjallajökull eruption in April 2010 – detection of volcanic plume using in-situ measurements, ozone sondes and lidar-ceilometer profiles, *Atmos. Chem. Phys.*, 10, 10085–10092, doi:10.5194/acp-10-10085-2010, 2010.
- Forster, C., Wandinger, U., Wotawa, G., James, P., Mattis, I., Althausen, D., Simmonds, P., O'Doherty, S., Jennings, S. G., Kleefeld, C., Schneider, J., Trickl, T., Kreipl, S., Jäger, H., and Stohl, A.: Transport of boreal forest fire emissions from Canada to Europe, *J. Geophys. Res.*, 106, 22887–22906, 2001.
- Fromm, M. and Servranckx, R.: Transport of forest fire smoke, above the tropopause, supercell convection, *Geophys. Res. Lett.*, 30, 1542, doi:10.1029/2002GL016820, 2003.
- Fromm, M., Alfred, J., Hoppel, K., Hornstein, J., Bevilacqua, R., Shettle, E., Servranckx, R., Li, Z., and Stocks, B.: Observations of boreal forest fire smoke in the stratosphere by POAM III, SAGE II, and lidar in 1998, *Geophys. Res. Lett.*, 27, 1407–1410, 2000.
- Fromm, M., Torres, O., Diner, D., Lindsey, D., Vant Hull, B., Servranckx, R., Shettle, E. P., and Li, Z.: Stratospheric impact of the Chisholm pyrocumulonimbus eruption: 1. Earth-viewing satellite perspective, *J. Geophys. Res.*, 113, D08202, doi:10.1029/2007JD009153, 2008a.
- Fromm, M., Shettle, E. P., Fricke, K. H., Ritter, C., Trickl, T., Giehl, H., Gerding, M., Barnes, J., O'Neill, M., Massie, S. T., Blum, U., McDermid, I. S., Leblanc, T., and Deshler, T.: The stratospheric impact of the Chisholm PyroCumulonimbus eruption: 2. Vertical profile perspective, *J. Geophys. Res.*, 113, D08203, doi:10.1029/2007JD009147, 2008b.
- Fromm, M., Lindsey, D. T., Servranckx, R., Yue, G., Trickl, T., Sica, R., Doucet, P., and Godin-Beekmann, S.: The Untold Story of Pyrocumulonimbus, *B. Am. Meteorol. Soc.*, 91, 1193–1209, 2010.
- Gregory, G. L., Browell, E. V., and Warren, L. S.: Boundary Layer Ozone: An Airborne Survey Above the Amazon Basin, *J. Geophys. Res.*, 93, 1452–1468, 1988.
- Gregory, G. L., Anderson, B. E., Warren, L. S., Browell, E. V., Bagwell, D. R., and Hudgins, C. H.: Tropospheric ozone and aerosol observations: The Alaskan Arctic, *J. Geophys. Res.*, 97, 16451–16471, 1992.
- Heese, B., Flentje, H., Althausen, D., Ansmann, A., and Frey, S.: Ceilometer lidar comparison: backscatter coefficient retrieval and signal-to-noise ratio determination, *Atmos. Meas. Tech.*, 3, 1763–1770, doi:10.5194/amt-3-1763-2010, 2010.
- Huntrieser, H., Heland, J., Schlager, H., Forster, C., Stohl, A., Aufmhoff, H., Arnold, F., Scheel, H. E., Campana, M., Gilge, S., Eixmann, R., and Cooper, O.: Intercontinental air pollution transport from North America to Europe: Experimental evidence from aircraft measurements and surface observations, *J. Geophys. Res.*, 110, D01305, doi:10.1029/2004JD005045, 2005.
- Jacob, D. J., Wofsy, S. C., Bakwin, P. S., Fan, S.-M., Harriss, R. C., Talbot, R. W., Bradshaw, J. D., Sandholm, S. T., Singh, H. B., Browell, E. V., Gregory, G. L., Sachse, G. W., Shipham, M. C., Blake, D. R., and Fitzjarrald, D. R.: Summertime Photochemistry of the Troposphere at High Northern Latitudes, *J. Geophys. Res.*, 97, 16421–16431, 1992.
- Jaffe, D. A. and Wigder, N. L.: Ozone production from wildfires: A critical review, *Atmos. Environ.*, 51, 1–10, 2012.
- Jonson, J. E., Simpson, D., Fagerli, H., and Solberg, S.: Can we explain the trends in European ozone levels?, *Atmos. Chem. Phys.*, 6, 51–66, doi:10.5194/acp-6-51-2006, 2006.
- Kempfer, U., Carnuth, W., Lotz, R., and Trickl, T.: A Wide-range UV Lidar System for Tropospheric Ozone Measurements: Development and Application, *Rev. Sci. Instrum.*, 65, 3145–3164, 1994.
- Kirchhoff, V. W. J. H.: Increasing Concentrations of CO and O<sub>3</sub>, *Environ. Sci. Pollut. Res.*, 3, 210–212, 1996.
- Kirchhoff, V. W. J. H. and Marinho, E. V. A.: Layer Enhancements of Tropospheric Ozone in Regions of Biomass Burning, *Atmos. Environ.*, 28, 69–74, 1994.
- Kirchhoff, V. W. J. H., Alves, J. R., and da Silva, F. R.: Observations of ozone concentrations in the Brazilian cerrado during the TRACE A field expedition, *J. Geophys. Res.*, 101, 24029–24042, 1996.
- Klett, J. D.: Lidar inversion with variable backscatter/extinction ratios, *Appl. Optics*, 24, 1638–1643, 1985.
- Logan, J. A., Staehelin, J., Megretskaia, I. A., Cammas, J.-P., Thouret, V., Claude, H., De Backer, H., Steinbacher, M., Scheel, H.-E., Stübi, R., Fröhlich, M., and Derwent, R.: Changes in ozone over Europe: Analysis of ozone measurements from sondes, regular aircraft (MOZAIC) and alpine surface sites, *J. Geophys. Res.*, 117, D09301, doi:10.1029/2011JD016952, 2012.
- Mattis, I., Ansmann, A., Wandinger, U., and Müller, D.: Unexpectedly high aerosol load in the free troposphere over central Europe in spring/summer 2003, *Geophys. Res. Lett.*, 30, 2178, doi:10.1029/2003GL018442, 2003.
- Mattis, I., Ansmann, A., Müller, D., Wandinger, U., and Althausen, D.: Multiyear aerosol observations with dual-wavelength Raman lidar in the framework of EARLINET, *J. Geophys. Res.*, 109, D13203, doi:10.1029/2004JD004600, 2004.
- Mauzerall, D. L., Jacob, D. J., Fan, S.-M., Bradshaw, J. D., Gregory, G. L., Sachse, G. W., and Blake, D. R.: Origin of tropospheric ozone in remote high northern latitudes in summer, *J. Geophys. Res.*, 101, 4175–4188, 1996.
- Methven, J., Arnold, S. R., Stohl, A., Evans, M. J., Avery, M., Law, K., Lewis, A. C., Monks, P. S., Parrish, D. D., Reeves, C. E., Schlager, H., Atlas, E., Blake, D. R., Coe, H., Crosier, J., Flocke, F. M., Holloway, J. S., Hopkins, J. R., McQuaid, J., Purvis, R., Rappenglück, B., Singh, H. B., Watson, N. M., Whalley, L. K., and Williams, P. I.: Establishing Lagrangian connections between observations within air masses crossing the Atlantic during the International Consortium for Atmospheric Research on Transport and Transformation experiment, *J. Geophys. Res.*, 111, D23S62, doi:10.1029/2006JD007540, 2006.
- Müller, D., Mattis, I., Wandinger, U., Ansmann, A., and Althausen, D.: Raman lidar observations of aged Siberian and Canadian forest fire smoke in the free troposphere over Germany in 2003: Microphysical particle characterization, *J. Geophys. Res.*, 110, D17201, doi:10.1029/2004JD005756, 2005.
- Müller, D., Mattis, I., Ansmann, A., Wandinger, U., Ritter, C., and Kaiser, D.: Multiwavelength Raman lidar observations of particle growth during long-range transport of forest-fire smoke in the free troposphere, *Geophys. Res. Lett.*, 34, L05803, doi:10.1029/2006GL027936, 2007.
- Oltmans, S. J., Lefohn, A. S., Shadwick, D., Harris, J. M., Scheel, H. E., Galbally, I., Tarasick, D. W., Johnson, B. J., Brunke, E.-G., Claude, H., Zeng, G., Nichol, S., Schmidlin, F., Davies, J.,

- Cuevas, E., Redondas, A., Naoe, H., Nakano, T., and Kawasato, T.: Recent tropospheric ozone changes – A pattern dominated by slow or no growth, *Atmos. Environ.*, 67, 331–351, 2012.
- Ordoñez, C., Brunner, D., Staehelin, J., Hadjinicolaou, P., Pyle, J. A., Jonas, M., Wernli, H., and Prévôt, A. S. H.: Strong influence of lowermost stratospheric ozone on lower tropospheric background ozone changes over Europe, *Geophys. Res. Lett.*, 34, L07805, doi:10.1029/2006GL029113, 2007.
- Pappalardo, G.: Lidar ratio data base, in: *EARLINET: A European Aerosol Research Lidar Network to Establish an Aerosol Climatology*, Final Report, European Union, edited by: Bösenberg, J. and Matthias, V., 148–151, Max-Planck-Institut für Meteorologie, Report No. 348 (Hamburg, Germany), ISSN 09371060, 2003.
- Parrish, D. D., Law, K. S., Staehelin, J., Derwent, R., Cooper, O. R., Tanimoto, H., Volz-Thomas, A., Gilge, S., Scheel, H.-E., Steinbacher, M., and Chan, E.: Long-term changes in lower tropospheric baseline ozone concentrations at northern mid-latitudes, *Atmos. Chem. Phys.*, 12, 11485–11504, doi:10.5194/acp-12-11485-2012, 2012.
- Petzold, A., Weinzierl, B., Huntrieser, H., Stohl, A., Real, E., Cozic, J., Fiebig, M., Hendricks, J., Lauer, A., Law, K., Roiger, A., Schlager, H., and Weingartner, E.: Perturbation of the European free troposphere aerosol by North American forest fire plumes during the ICARTT-ITOP experiment in summer 2004, *Atmos. Chem. Phys.*, 7, 5105–5127, doi:10.5194/acp-7-5105-2007, 2007.
- Real, E., Law, K. S., Weinzierl, B., Fiebig, M., Petzold, A., Wild, O., Methven, J., Arnold, S., Stohl, A., Huntrieser, H., Roiger, A., Schlager, H., Stewart, D., Avery, M., Sachse, G., Brownell, E., Ferrare, R., and Blake, D.: Processes influencing ozone levels in Alaskan forest fire plumes during long-range transport over the North Atlantic, *J. Geophys. Res.*, 112, D10S41, doi:10.1029/2006JD007576, 2007.
- Richardson, J. L., Fishman, J., and Gregory, G. L.: Ozone Budget Over the Amazon, Regional Effects From Biomass-Burning Emissions, *J. Geophys. Res.*, 96, 13073–13087, 1991.
- Roelofs, G.-J. and Lelieveld, J.: Model study of the influence of cross-tropopause O<sub>3</sub> transports on tropospheric O<sub>3</sub> levels, *Tellus B*, 49, 38–55, 1997.
- Roelofs, G. J., Kentarchos, A. S., Trickl, T., Stohl, A., Collins, W. J., Crowther, R. A., Hauglustaine, D., Klonecki, A., Law, K. S., Lawrence, M. G., von Kuhlmann, R., and van Weele, M.: Intercomparison of tropospheric ozone models: Ozone transport in a complex tropopause folding event, *J. Geophys. Res.*, 108, 8529, doi:10.1029/2003JD003462, 2003.
- Scheel, H. E.: Ozone Climatology Studies for the Zugspitze and Neighbouring Sites in the German Alps, in: *Tropospheric Ozone Research 2, EUROTRAC-2 Subproject Final Report*, edited by: Lindskog, A., pp. 134–139, EUROTRAC International Scientific Secretariat, München, Germany, available at: <http://www.trickl.de/scheel.pdf> (last access: 26 August 2015), 2003.
- Scheel, H. E.: Ozon, in: *ATMOFAST*, available at: <http://www.trickl.de/ATMOFAST.htm> (last access: 26 August 2015), 66–71, 2005.
- Seibert, P., Feldmann, H., Neining, B., Bäumle, M., and Trickl, T.: South foehn and ozone in the Eastern Alps – case study and climatological aspect, *Atmos. Environ.*, 34, 1379–1394, 2000.
- Škerlak, B., Sprenger, M., and Wernli, H.: A global climatology of stratosphere–troposphere exchange using the ERA-Interim data set from 1979 to 2011, *Atmos. Chem. Phys.*, 14, 913–937, doi:10.5194/acp-14-913-2014, 2014.
- Sprenger, M., Croci Maspoli, M., and Wernli, H.: Tropopause folds and cross-tropopause exchange: A global investigation based upon ECMWF analyses for the time period March 2000 to February 2001, *J. Geophys. Res.*, 108, 8518, doi:10.1029/2002JD002587, 2003.
- Stohl, A. and Seibert, P.: Accuracy of trajectories as determined from the conservation of meteorological tracers, *Q. J. Roy. Meteorol. Soc.*, 124, 1465–1484, 1998.
- Stohl, A. and Trickl, T.: A textbook example of long-range transport: Simultaneous observation of ozone maxima of stratospheric and North American origin in the free troposphere over Europe, *J. Geophys. Res.*, 104, 30445–30462, 1999.
- Stohl, A., Spichtinger-Rakowsky, N., Bonasoni, P., Feldmann, H., Memmesheimer, M., Scheel, H. E., Trickl, T., Hübener, S., Ringer, W., and Mandl, M.: The influence of stratospheric intrusions on alpine ozone concentrations, *Atmos. Environ.*, 34, 1323–1354, 2000.
- Stohl, A., Eckhardt, S., Spichtinger, N., Huntrieser, H., Heiland, J., Schlager, H., Wilhelm, S., Arnold, F., and Cooper, O.: A backward modelling study of intercontinental transport using aircraft measurements, *J. Geophys. Res.*, 108, 4370, doi:10.1029/2002JD002862, 2003.
- Trickl, T., Cooper, O. C., Eisele, H., James, P., Mücke, R., and Stohl, A.: Intercontinental transport and its influence on the ozone concentrations over central Europe: Three case studies, *J. Geophys. Res.*, 108, 8530, doi:10.1029/2002JD002735, 2003.
- Trickl, T., Feldmann, H., Kanter, H.-J., Scheel, H.-E., Sprenger, M., Stohl, A., and Wernli, H.: Forecasted deep stratospheric intrusions over Central Europe: case studies and climatologies, *Atmos. Chem. Phys.*, 10, 499–524, doi:10.5194/acp-10-499-2010, 2010.
- Trickl, T., Bärtsch-Ritter, N., Eisele, H., Furger, M., Mücke, R., Sprenger, M., and Stohl, A.: High-ozone layers in the middle and upper troposphere above Central Europe: potential import from the stratosphere along the subtropical jet stream, *Atmos. Chem. Phys.*, 11, 9343–9366, doi:10.5194/acp-11-9343-2011, 2011.
- Trickl, T., Giehl, H., Jäger, H., and Vogelmann, H.: 35 yr of stratospheric aerosol measurements at Garmisch-Partenkirchen: from Fuego to Eyjafjallajökull, and beyond, *Atmos. Chem. Phys.*, 13, 5205–5225, doi:10.5194/acp-13-5205-2013, 2013.
- Trickl, T., Vogelmann, H., Giehl, H., Scheel, H.-E., Sprenger, M., and Stohl, A.: How stratospheric are deep stratospheric intrusions?, *Atmos. Chem. Phys.*, 14, 9941–9961, doi:10.5194/acp-14-9941-2014, 2014.
- Val Martin, M., Honrath, R. E., Owen, R. C., Pfister, G., Fialho, P., and Barata, F.: Significant enhancements of nitrogen oxides, black carbon, and ozone in the North Atlantic lower free troposphere resulting from North American boreal wild fires, *J. Geophys. Res.*, 111, D23S60, doi:10.1029/2006JD007530, 2006.
- Vautard, R., Szopa, S., Beekmann, M., Menut, L., Hauglustaine, D. A., Rouil, L., and Roemer, M.: Are decadal anthropogenic emission reductions in Europe consistent with surface ozone observations?, *Geophys. Res. Lett.*, 33, L13810, doi:10.1029/2006GL026080, 2006.

- VDI (Verein Deutscher Ingenieure): Guideline VDI 3786, Part 15, Environmental meteorology, ground-based remote sensing of visual range, visual-range lidar, Düsseldorf, Germany, 32 pp., 2004.
- Verma, S., Worden, J., Pierce, B., Jones, D. B. A., Al-Saadi, J., Boersma, F., Bowman, K., Elderling, A., Fisher, B., Jourdain, L., Kulawik, S., and Worden, H.: Ozone production in boreal fire smoke plumes using observations from the Tropospheric Emission Spectrometer and the Ozone Monitoring Instrument, *J. Geophys. Res.*, 114, D02303, doi:10.1029/2008JD010108, 2009.
- Vogelmann, H. and Trickl, T.: Wide-Range Sounding of Free-Tropospheric Water Vapor with a Differential-Absorption Lidar (DIAL) at a High-Altitude Station, *Appl. Optics*, 47, 2116–2132, 2008.
- Vogelmann, H., Sussmann, R., Trickl, T., and Borsdorff, T.: Intercomparison of atmospheric water vapor soundings from the differential absorption lidar (DIAL) and the solar FTIR system on Mt. Zugspitze, *Atmos. Meas. Tech.*, 4, 835–841, doi:10.5194/amt-4-835-2011, 2011.
- Vogelmann, H., Sussmann, R., Trickl, T., and Reichert, A.: Spatiotemporal variability of water vapor investigated using lidar and FTIR vertical soundings above the Zugspitze, *Atmos. Chem. Phys.*, 15, 3135–3148, doi:10.5194/acp-15-3135-2015, 2015.
- Völger, P., Bösenberg, J., and Schult, I.: Scattering Properties of Selected Model Aerosols Calculated at UV-Wavelengths: Implications for DIAL Measurements of Tropospheric Ozone, *Beitr. Phys. Atmosph.*, 69, 177–187, 1996.
- Wiegner, M. and Geiß, A.: Aerosol profiling with the Jenoptik ceilometer CHM15kx, *Atmos. Meas. Tech.*, 5, 1953–1964, doi:10.5194/amt-5-1953-2012, 2012.
- Wirth, M., Fix, A., Ehret, G., Reichardt, J., Begie, R., Engelbart, D., Vömel, H., Calpini, B., Romanens, G., Apituley, A., Wilson, K. M., Vogelmann, H., and Trickl, T.: Intercomparison of Airborne Water Vapour DIAL Measurements with Ground Based Remote Sensing and Radiosondes within the Framework of LU-AMI 2008, Contribution S07-P01-1, in: Proceedings of the 8th International Symposium on Tropospheric Profiling (ISTP2009), Delft (the Netherlands), 19–23 October 2009, edited by: Apituley, A., Russchenberg, H. W. J., and Monna, W. A. A., 3 pp., RIVM, the Netherlands, available at: <http://cerberus.rivm.nl/ISTP/pages/index.htm>, ISBN 978-90-6960-233-2, 2009.
- Wofsy, S. C., Sachse, G. W., Gregory, G. L., Blake, D. R., Bradshaw, J. D., Sandholm, S. T., Singh, H. B., Barrick, J. A., Harris, R. C., Talbot, R. W., Shipham, M. A., Browell, E. V., Jacob, D. J., and Logan, J. A.: Atmospheric Chemistry in the Arctic and Subarctic: Influence of Natural Fires, Industrial Emissions, and Stratospheric Inputs, *J. Geophys. Res.*, 97, 16731–16746, 1992.
- Wotawa, G. and Trainer, M.: The Influence of Canadian Forest Fires on Pollutant Concentrations in the United States, *Science*, 288, 324–328, 2000.
- Zanis, P., Trickl, T., Stohl, A., Wernli, H., Cooper, O., Zerefos, C., Gaeggeler, H., Schnabel, C., Tobler, L., Kubik, P. W., Priller, A., Scheel, H. E., Kanter, H. J., Cristofanelli, P., Forster, C., James, P., Gerasopoulos, E., Delcloo, A., Papayannis, A., and Claude, H.: Forecast, observation and modelling of a deep stratospheric intrusion event over Europe, *Atmos. Chem. Phys.*, 3, 763–777, doi:10.5194/acp-3-763-2003, 2003.